



Oct 24 – 26, 2022
Napoli, Italy

IV Geant4 International User Conference at the physics-medicine-biology frontier

Internal dosimetry of salivary glands in PSMA-targeted PET/CT: a Monte Carlo based study

Daniele Pistone^{1,2}, Lucrezia Auditore^{1,2}, Antonio Italiano^{2,3}, Silvano Gnesin⁴, Francesco Cicone^{5,6}, Giuseppe Lucio Cascini^{5,6}, Ernesto Amato^{1,2}

¹ BIOMORF Department, University of Messina, Italy

² INFN, Section of Catania, Italy

³ MIFT Department, University of Messina, Italy

⁴ IRA, Lausanne University Hospital and University of Lausanne, Switzerland

⁵ Dep. of Experimental and Clinical Medicine, “Magna Graecia” University of Catanzaro, Italy

⁶ Nuclear Medicine Unit, University Hospital “Mater Domini”, Catanzaro, Italy



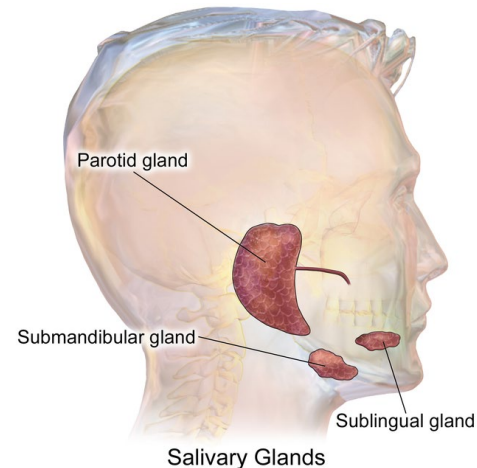
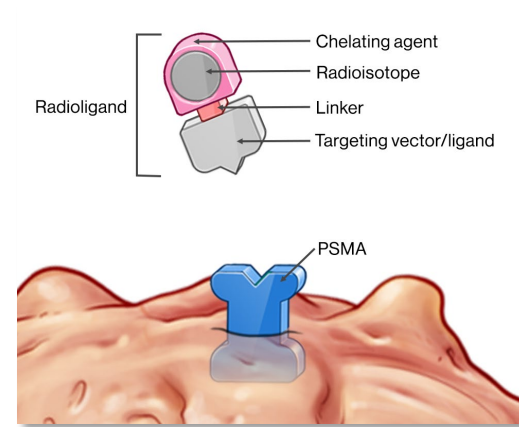
Università
degli Studi di
Messina



Unil
UNIL | Université de Lausanne

Context

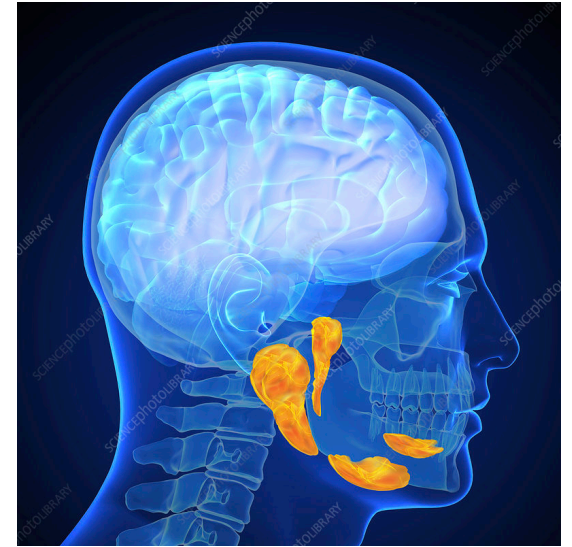
- Prostate-Specific Membrane Antigen (PSMA) radiolabelled ligands are used for diagnosis and therapy of prostate cancer
- Salivary glands (SGs) also exhibit high PSMA-ligands uptake → are the dose-limiting organ in PSMA-targeted therapies
- SG dosimetry is usually performed adopting simplified approaches (e.g. organ-level MIRD) and approximated geometries (e.g. SGs treated as a unique organ)



Boxtel et al. 2020
Theranostics **10** 2273-2283

Aim of the study

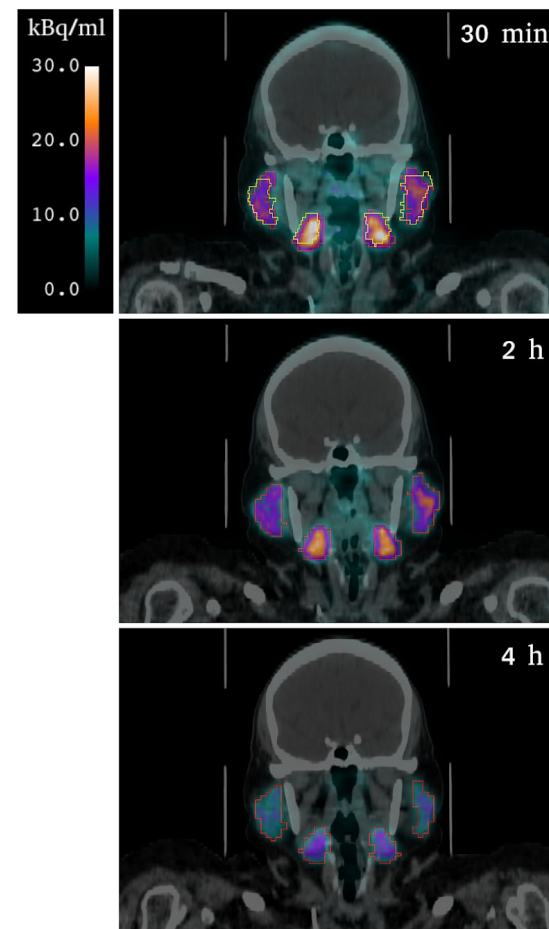
- Perform 3D voxel-level patient-specific dosimetry of salivary glands ^{18}F -PSMA-1007 PET/CT:
 - Separately for **left** and **right parotids** and **submandibular glands**
 - Using GATE/GEANT4 direct Monte Carlo simulations with tomographic imaging as input
- Compare with other simplified dosimetric methods:
 - Spherical method of OLINDA/EXM 2.1
 - Ellipsoidal method by Amato et al. [1]
 - MIRDA approach with OLINDA's and OpenDose's organ-level S-factors



[1] Amato et al. 2014 *AAPP* **92**(1) A1, <https://doi.org/10.1478/AAPP.921A1>

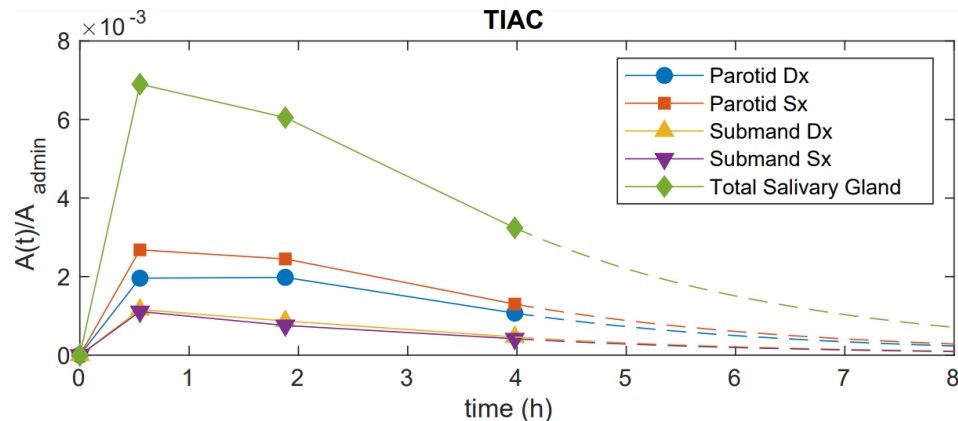
Patient data

- 5 patients with prostate cancer recurrences enrolled (“Mater Domini” Hospital of Catanzaro, Italy)
- Each one underwent 3 sequential PET/CTs of head-neck at 30 min, 2 h and 4 h after ^{18}F -PSMA-1007 injection

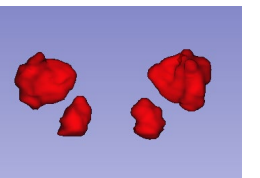
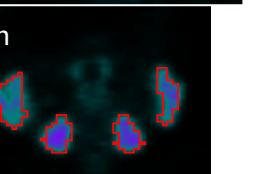
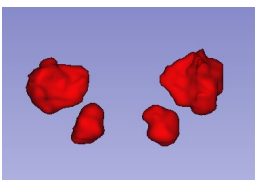
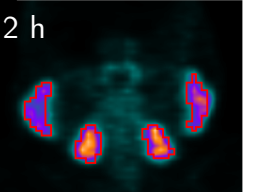
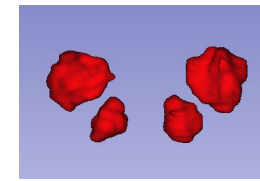
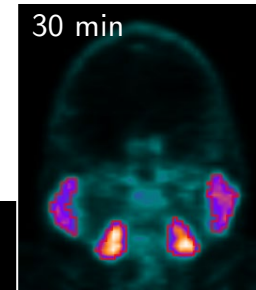
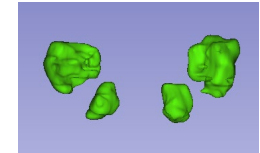
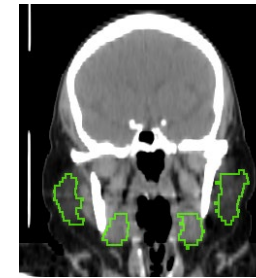


VOIs segmentation and time-activity analysis

- **Morphologic VOIs segmentation** on 30 min CT (manual)
 - → vol. and mass of SGs (density $1.045 \text{ g}\cdot\text{cm}^{-3}$ from ICRP 89)
- **Functional VOIs segmentation** on each ^{18}F -PSMA-1007 PET (thresholding: 25% of the max $A(t)$ in SGs [2])
 - For simplified methods:
 - → total normalized activity ($A(t)/A_{\text{admin}}$) in each VOI
 - → Time-Integrated Activity Coefficients (TIACs) via trapezoid + physical decay tail integration

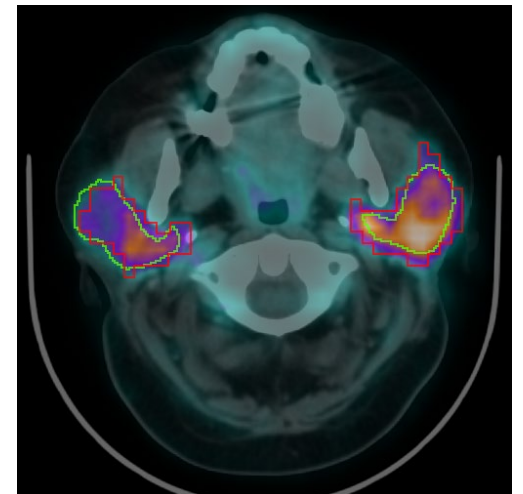
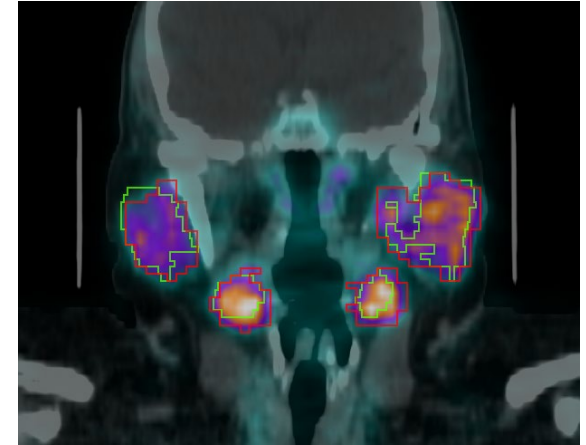


[2] Hobbs et al. 2013 *Q J Nucl Med Mol Imaging* 57(1) 79–91



VOIs segmentation and time-activity analysis

- **Morphologic VOIs segmentation** on 30 min CT (manual)
 - → vol. and mass of SGs (density $1.045 \text{ g}\cdot\text{cm}^{-3}$ from ICRP 89)
- **Functional VOIs segmentation** on each ^{18}F -PSMA-1007 PET (thresholding: 25% of the max $A(t)$ in SGs [2])
 - For simplified methods:
 - → total normalized activity ($A(t)/A_{\text{admin}}$) in each VOI
 - → Time-Integrated Activity Coefficients (TIACs) via trapezoid + physical decay tail integration
- Purpose:
 - Take into account activity spill-out and non-optimal spatial matching of PET activity distribution with respect to CT morphology

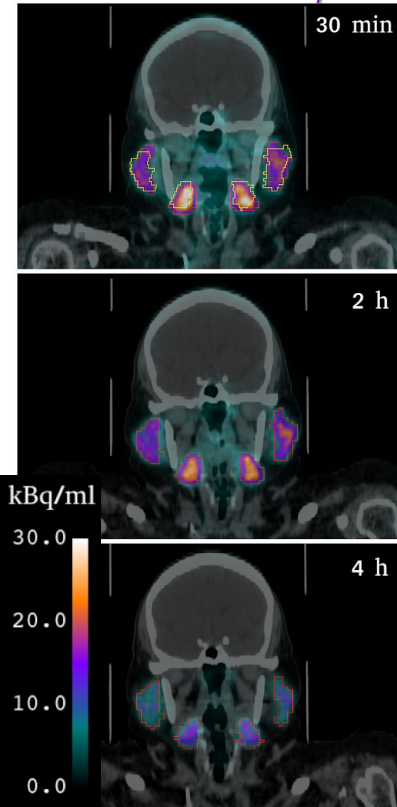


[2] Hobbs et al. 2013 *Q J Nucl Med Mol Imaging* **57**(1) 79–91

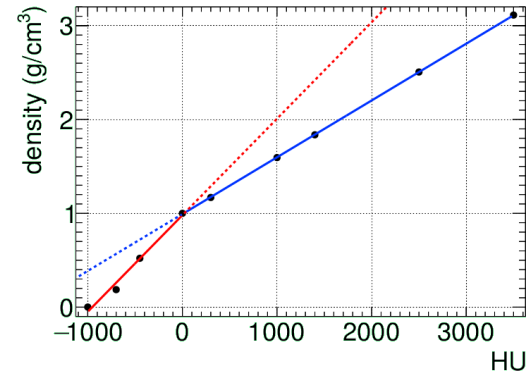
GATE/GEANT4 Monte Carlo simulations (1/3)

Monte Carlo simulations with GATE 9.1 (GEANT4 10.7) using tomographic imaging as input

- CT → voxelized phantom of patient's body: HU to density conversion via *Automated HU stoichiometric calibration* according to [3], *density tolerance* of 0.01 g/cm^3 , materials in Tab.
- PET → radionuclide (^{18}F) spatial decay probability via *linear translator* of *imageReader*



G4 Materials (ICRP)	HU intervals	ρ (g/cm^3)
AIR	$\text{HU} \leq -900$	$\rho \leq 0.10$
LUNG	$-900 < \text{HU} \leq -150$	$0.10 < \rho \leq 0.85$
ADIPOSE_TIS.	$-150 < \text{HU} \leq -50$	$0.85 < \rho \leq 0.94$
SOFT_TIS.	$-50 < \text{HU} \leq 290$	$0.94 < \rho \leq 1.2$
BONE_CORT.	$\text{HU} > 290$	$\rho > 1.2$



[3] Schneider et al. 2000 *Phys Med Biol* **45** 459-478

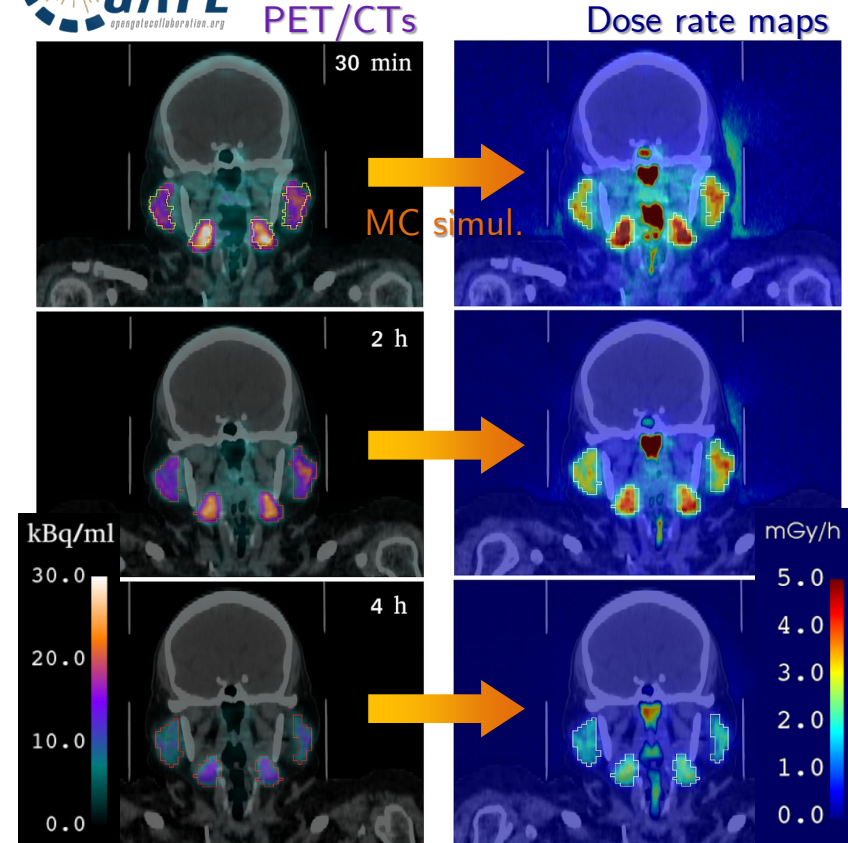
GATE/GEANT4 Monte Carlo simulations (2/3)

Monte Carlo simulations with GATE 9.1 (GEANT4 10.7) using tomographic imaging as input



- Simulations settings:
 - ^{18}F decays: *G4RadioactiveDecay*
 - Physics List: *G4EmStandard_opt4*
 - range cuts: 0.1 mm
 - absorbed dose scoring: *DoseActor* with *MassWeighting* algorithm, CT resolution
 - $N_{evts} = 2 \cdot 10^8$ for each simulation
- For each time-point: absorbed dose rate ($\dot{D}(t)$) map

$$\dot{D}^{ijk}(t) = D_{MC}^{ijk}(t) \cdot A_{FOV\ PET}(t) / N_{evts}$$



GATE/GEANT4 Monte Carlo simulations (3/3)

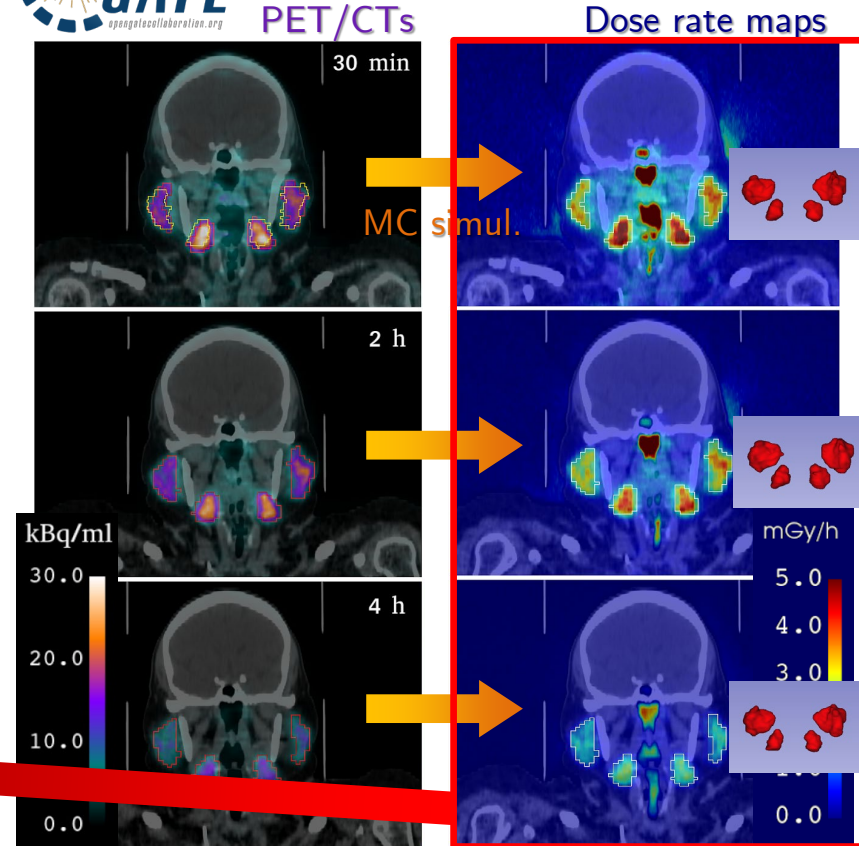
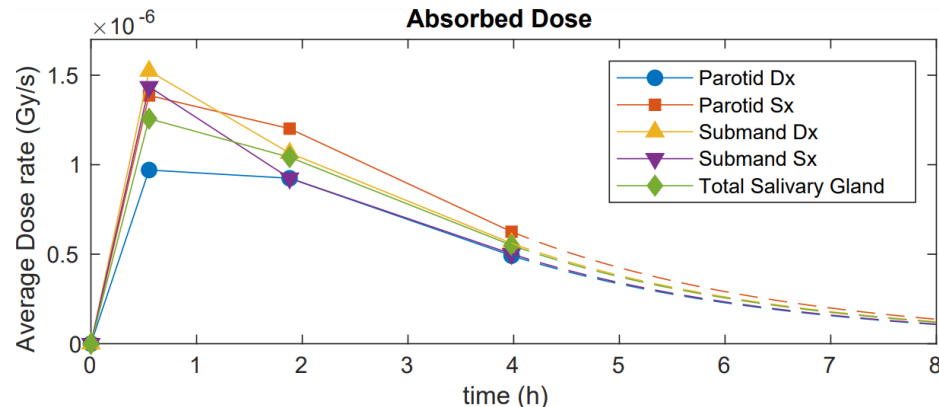
Monte Carlo simulations with GATE 9.1 (GEANT4 10.7) using tomographic imaging as input



- Average $\dot{D}(t)$ calculated in **SG functional VOIs** (with possible air and bone voxels excluded) + applying **corrective factor for mass**:

$$\langle \dot{D}(t) \rangle_{gland} = \langle \dot{D}^{ijk}(t) \rangle_{funct\ VOI} \cdot (Vol_{funct\ VOI} / Vol_{morph\ VOI})$$

- Average D via trapezoid + phys. decay tail integr.



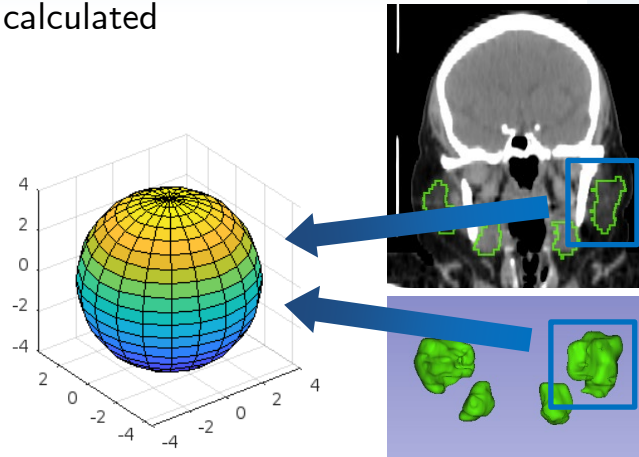
Simplified dosimetric methods for comparison (1/2)

- **(SM)** Spherical method of OLINDA/EXM 2.1
- **(EM)** Ellipsoidal method by Amato et al. [1]

- Calculates average self absorbed dose ($\langle D \rangle$) to sphere of homogeneous material and density and uniform activity
- Each SG treated as individual sphere of soft tissue
- Volume and mass adjusted to patient's ones from morphologic segmentations
- TIACs deduced from ^{18}F -PSMA-1007 PETs entered in the software for each gland
- → Average absorbed dose to each SG and to union of the four glands (tSG) calculated

$$\langle D \rangle_{tSG} = \frac{\sum_i m_i \langle D \rangle_i}{\sum_i m_i}$$

i = individual SG

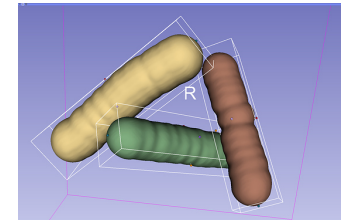
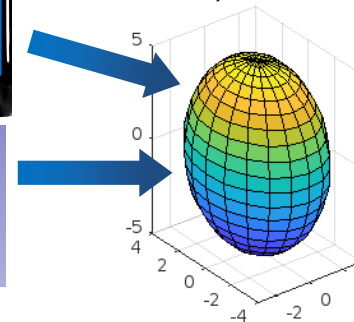


- Similar to spherical method but using ellipsoids
- Analytic model, from GEANT4 simul., implemented on spreadsheet employing emission spectrum of radionuclide (from <http://www.doseinfo-radar.com/>)
- Inputs: ellipsoid axes, density, TIAC, injected activity
- Ellipsoids' axes deduced exploiting 3D Slicer:

- *Labelmap statistics* tool → Oriented Bounding Box diameters ($OBBd$) of the SG VOIs → actual axes (a) deduced as:

$$a = OBBd \cdot \sqrt[3]{Vol_{OBB\ ellipsoid} / Vol_{morph\ VOI}}$$

- → implemented ellipsoid has same volume (and mass) as that of the morphologic gland



OBB = smallest non-axis aligned box encompassing a VOI

[1] Amato et al. 2014 *AAPP* 92(1) A1, <https://doi.org/10.1478/AAPP.921A1>

Simplified dosimetric methods for comparison (2/2)

➤ Organ S-Factors MIRD approach

- Average absorbed dose to tSG following the organ-level MIRD formalism:

$$D_{(T \leftarrow S)} = S_{(T \leftarrow S)} \cdot A_{adm} \cdot TIAC_{(S)} \quad \begin{array}{l} S = \text{source} \\ T = \text{target} \end{array}$$
$$S_{(T \leftarrow S)} = \sum_i y_i E_i \Phi_{i(T \leftarrow S)}$$

where Φ_i = Specific Absorbed Fraction (SAF, kg^{-1}), y_i = yield ($\text{Bq}^{-1}\cdot\text{s}^{-1}$) and E_i = energy (J) for radiation type i

- Using the S-factors provided by:
- **(S-O)** OLINDA/EXM 2.1: calculated with NURBS voxel-based adult male phantom adjusted to ICRP 89 masses [4]
- **(S-OD)** OpenDose collaboration: calculated with ICRP 110 voxel-based adult male phantom [5,6]

- The following source-target setups were investigated:

OLINDA

- **S-O1:** tSG only source and target
- **S-O2:** S-O1 + additional contrib. of remainder of body (RB) as source, using $TIAC_{RB} = TIAC_{WB} - TIAC_{tSG}$, with $TIAC_{WB} = 2.64 \text{ h } (^{18}\text{F}'\text{s } \tau)$ [7] (in absence of whole-body imaging, assumption of phys. dec. only, no bio. wash-out)

OpenDose

- **S-OD1:** tSG only source and target
- **S-OD2:** same as S-O2 with OpenDose S-fact.
- **S-OD3:** S-O1 + additional contrib. of remainder of head (RH) as source, deducing $TIAC_{RH} = TIAC_{PET\text{ FOV}} - TIAC_{tSG}$ from scans (as in slide 4)
- In all the cases, correction for mass applied $\langle D \rangle_{tSG} = D_{(T \leftarrow S)} \cdot (m_{tSG\text{ phantom}}/m_{tSG\text{ patient}})$



tSG



RH



RB

Coronal view of OpenDose source organs adopted

[4] Stabin and Siegel 2018 *J Nucl Med* **59** 154–160 <https://doi.org/10.2967/jnumed.117.196261>

[5] Chauvin et al 2020 *J Nucl Med* **61**(10) 1514–1519 <https://doi.org/10.2967/jnumed.119.240366>

[6] <https://www.opendose.org/> [7] Giesel et al 2017 *Eur J Nucl Med Mol Imaging* **44**(4) 678–688 <https://doi.org/10.1007/s00259-016-3573-4>

Results: MC vs simplified methods, total SG VOI

For total salivary gland VOI:

- All methods except S-OD2 underestimate w.r.t MC
- Average relative percent differences (ϵ) and standard deviation (SD) among patients:

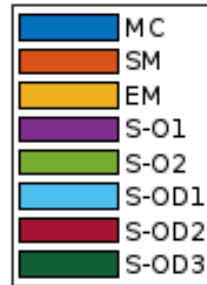
$$\epsilon_X = 100 \cdot \frac{\langle D \rangle_X - \langle D \rangle_{MC}}{\langle D \rangle_{MC}}$$

X = simplified *dosimetric method*

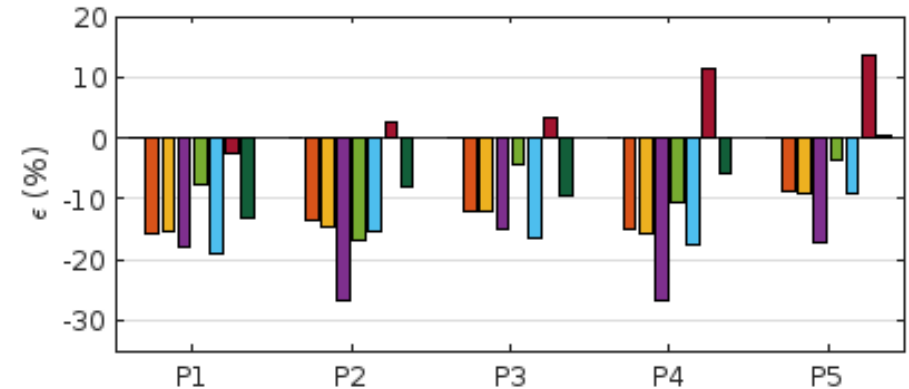
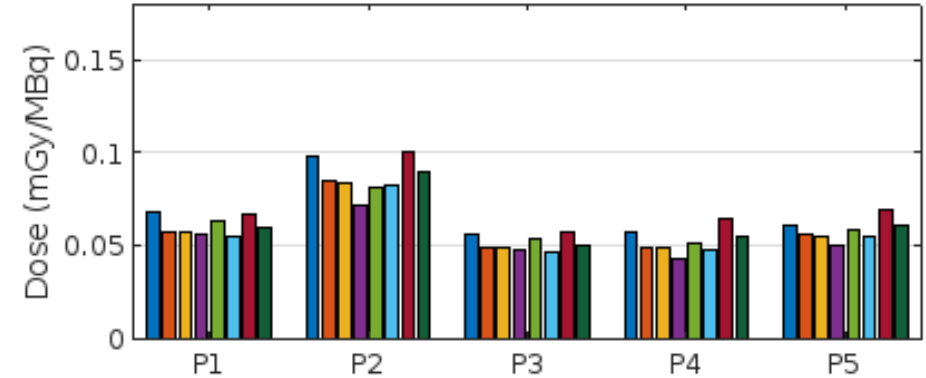
method	$\langle \epsilon \rangle$	SD
SM	-13.0	2.8
EM	-13.4	2.9
S-O1	-20.7	5.4
S-O2	-8.6	5.3
S-OD1	-15.5	3.7
S-OD2	5.7	6.6
S-OD3	-7.2	5.0

Causes of discrepancies w.r.t. MC

- No cross-dose from activity outside glands (SM, EM, S-O1, S-OD1)
- Simplified gland geometry (SM, EM)
- Different voxel geometries in anthropomorphic phantoms w.r.t. patient (S-O and S-OD)
- Uniform activity within the glands (all)



total Salivary Gland VOI



Results: MC vs simplified methods, individual SGs

For individual salivary glands:

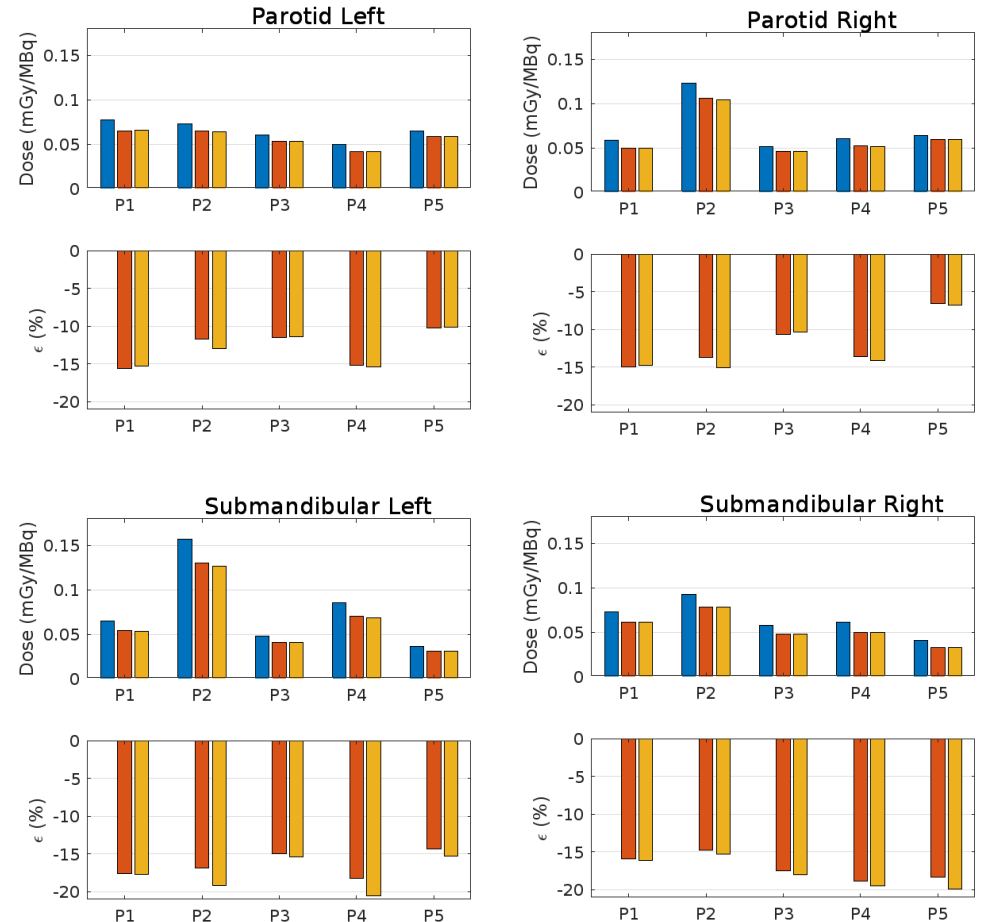
- Both spherical method (SM) and ellipsoidal method (EM) underestimate w.r.t. MC, between -20% and -6%
- Average relative percent differences (ϵ) and standard deviation (SD) among patients:
 - $\langle \epsilon \rangle_{SM} = -14.5\%$, $SD_{SM} = 3.2$
 - $\langle \epsilon \rangle_{EM} = -15.1\%$, $SD_{EM} = 3.6$

Causes of discrepancies w.r.t. MC

- no cross-dose from activity outside glands
- simplified geometry of the glands
- uniform activity within the glands

$$\epsilon_X = 100 \cdot \frac{\langle D \rangle_X - \langle D \rangle_{MC}}{\langle D \rangle_{MC}}$$

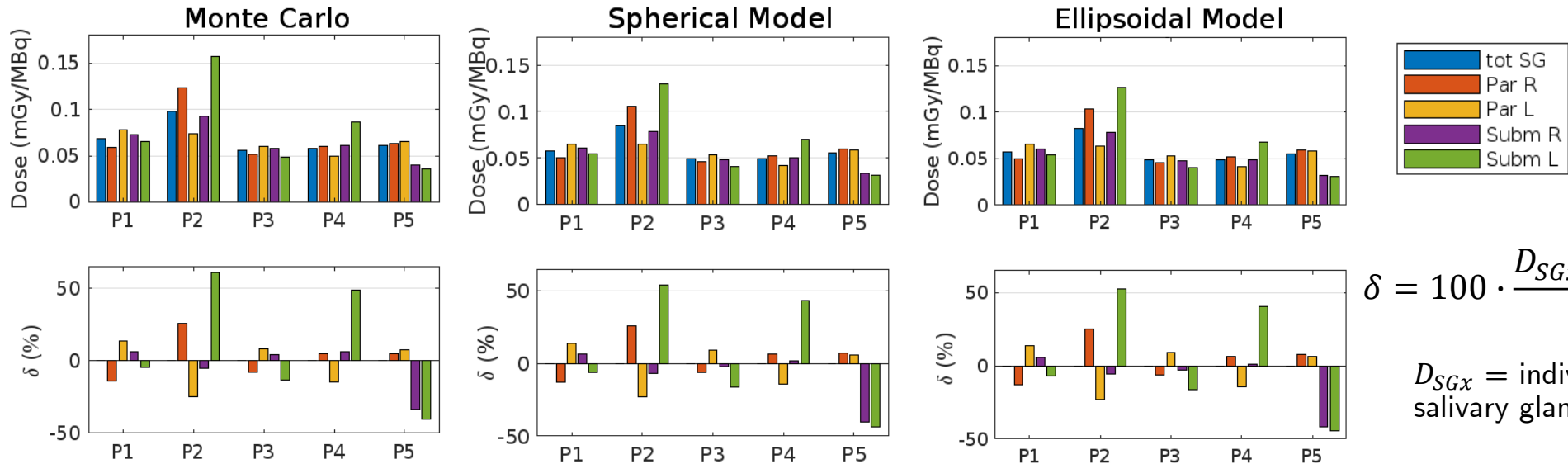
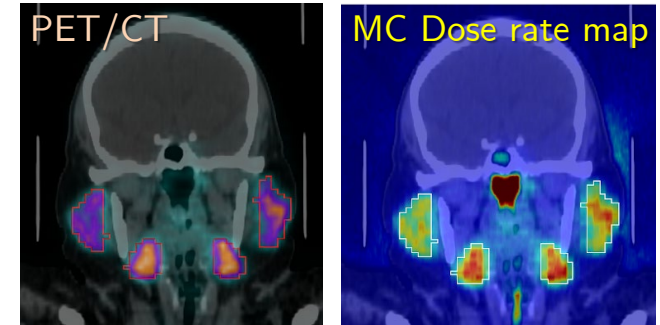
X = simplified *dosimetric method*



Results: comparison among individual SGs

For each method enabling dose estimation for individual SGs (MC, SM, EM):

- Non-negligible differences of absorbed dose in individual salivary glands
- Differences with respect to tSG between -50% and +65% with high intra- and inter-patient variability



$$\delta = 100 \cdot \frac{D_{SGx} - D_{tSG}}{D_{SGx}}$$

D_{SGx} = individual salivary gland x

Conclusions and perspectives

- General trend: simplified methods underestimate absorbed dose in salivary glands (SGs) with respect to MC for ^{18}F -PSMA PET dosimetry (except for method S-OD2)
- Average discrepancies w.r.t MC within 10% only with methods accounting for cross-dose from activity outside glands (S-O2, S-OD2, S-OD3)
- MC and methods enabling dosimetry for individual SGs (SM, EM) highlight patient-specific heterogeneous dose distribution in the four SGs considered (parotids and submandibular) → considering only “total SG” can be a strong approximation (overestimating or underestimating dose to individual SGs)
- Studies continuing on ^{18}F -PSMA-1007 dosimetry, trying to quantify the contribution of the different causes of discrepancies w.r.t. MC:
 - patient’s SGs masses w.r.t. standardized masses, cross-dose from activity outside glands, simplified geometry of the glands, uniform activity within the glands
- Future perspectives: extend this kind of study to therapeutic radionuclides and radiopharmaceuticals
- Paper containing the reported study currently under review, provisional version on arXiv: <https://doi.org/10.48550/arXiv.2210.01616>

Acknowledgements

- We acknowledge the CINECA award under the ISCRA initiative, for the availability of high performance computing resources and support (MIRACLE project, Marconi100 and Galileo100 supercomputers)
- Special thanks to all the colleagues collaborating in this study, from:
 - University of Messina and INFN Catania: Prof. Ernesto Amato, Dr. Lucrezia Auditore, Dr. Antonio Italiano
 - University of Catanzaro: Dr. Francesco Cicone, Prof. Giuseppe Lucio Cascini
 - University of Lausanne and CHUV: Dr. Silvano Gnesin



Università
degli Studi di
Messina



UMG
Dubium sapientiae initium

Unil

UNIL | Université de Lausanne



THANK YOU FOR YOUR ATTENTION!

Daniele Pistone, PhD
email: daniele.pistone@unime.it



Università
degli Studi di
Messina

